Reaction kinetics during early hydration of calcined phyllosilicates in model cement systems

Sebastian Scherb[a]*, Matthias Maier[b], Mathias, Köberl[a], Nancy Beuntner[a], Karl-Christian Thienel[a],

[a]*Civil Engineering and Environmental Science, University of the Bundeswehr Munich, Werner-Heisenberg-Weg 39, 85579 Neubiberg, Germany*

[b]*Group for Sustainable Binders, Fraunhofer IBP, Fraunhoferstr. 10, 83626 Valley*

sebastian.scherb@unibw.de, matthias.maier@ibp.fraunhofer.de, mathias.koeberl@unibw.de, nancy.beuntner@unibw.de, christian.thienel@unibw.de

*corresponding author

Abstract: Model cement systems form the basis for the systematic investigation of three calcined phyllosilicates. Metamuscovite acts as pure filler, accelerates alite hydration and leads to an increased degree of hydration of alite compared to the reference. A different picture emerges for metaillite and metakaolin. Despite the slight filler effect of the clay particles, the alite at the onset of the aluminate clinker reaction as well as after 2 days of hydration reaches significantly lower degrees of hydration. This indicates interaction of the negatively charged calcined clay surfaces with the sulfate from the pore solution. The chemical reactivity of the metaillite and metakaolin during early hydration can be demonstrated by direct quantification as well as by the consumption of portlandite and the formation of C-S-H. This leads to a better understanding of the effect of individual calcined phyllosilicates and help to predict the influence of complex calcined clays on early hydration.

Keywords: calcined clay; supplementary cementitious material; reaction kinetics; calorimetry; in situ X-ray diffraction

1. Introduction

Calcined clays (CC) are among the most promising materials to meet the increasing demand for clinker-reduced binders, as they are globally and locally available in sufficient quantities

and qualities [1]. The mineralogical complexity as well as complex surface properties of CC are a challenge in predicting their influence on early hydration [2, 3]. An improved understanding of the mechanisms behind the influence of calcined clays on early hydration is essential for their widespread use in modern cements and concretes and has a high potential for saving CO_2 [4].

Both, the mechanisms behind the influence of CC on the silicate as well as aluminate clinker reaction are currently under discussion and focus in case of the latter on the influence of different supplementary cementitious materials (SCMs) on the sulfate balance. Different theories are described regarding the impact on sulfate carrier dissolution and thus to an influence on the aluminate clinker reaction. All theories unite that adsorption effects on the surfaces of the C_3A particles [5], on the surfaces of the formed calcium silicate hydrate (C-S-H) phases [6, 7] or on the surfaces of the SCMs directly [8-10] influence the sulfate balance. According to their results, the reactivity of the SCMs used plays a minor role for the early hydration [7, 10]. Nevertheless, studies in clinker-free model systems show that both metakaolin (MK) and metaillite (MI) can independently form hydrate phases at very early times. Metamuscovite (MM) shows only a very low reactivity [9]. The relationship between the formation of the C-S-H and the dissolution of the sulfate carrier is well established for pure cement systems [7, 11, 12]. Thus, the influence of the aluminate clinker reaction, which is controlled by the dissolution of the sulfate carrier, is strongly dependent on alite reaction and the formation of C-S-H. This is also shown for the filler effect by the use of different SCMs. An accelerated alite hydration and consequently C-S-H formation accelerate the dissolution of the sulfate carrier [13]. Maier et al. [10] confirm this relationship in their reference systems and systems with limestone powder as filler. However, the results for CC with different kaolinite contents show that, in addition to the surfaces of the C-S-H, further surfaces are needed to completely adsorb the sulfate. In addition Jansen et al. [14] proved with a complete mass

balance approach that after the sulfate depletion, all sulfate is bound in ettringite (AFt). Thus, regardless of the mechanism and surfaces responsible for sulfate carrier dissolution and adsorption, desorption must occur to be available for reaction to AFt. Clearly sharper aluminate peaks during calorimetric measurements indicate differences of the desorption behavior and faster desorption of sulfate from metakaolin particles in comparison to C-S-H surfaces [10]. Investigations on CC with a high metaillite respectively metakaolin content show a clear influence, in particular on the sulfation of the systems depending on the meta-phyllosilicate used [8].

Despite great progress in understanding the mechanism of CC in cementitious systems, their mechanisms remain a subject of current debate. The complexity of the investigations with two multiphase mixtures, cement and clay, make the differentiation of physical and chemical effects very difficult. A reduction of the system to the clinker phases, which are decisive for the early hydration, as well as possible pure-phase meta-phyllosilicates form the basis and the starting point for the present work. The complete quantification of in situ X-ray diffraction (XRD) measurements during the first 50 h yield information on the influence of three individual, nearly pure calcined phyllosilicates ("meta-phyllosilicates": metakaolin, metaillite and metamuscovite) on the early clinker hydration of a synthetic cement system. By reducing the cement to the fast clinker phases alite and C_3A, aims to answer questions on the influence of individual meta-phyllosilicates on the silicate and aluminate clinker reaction as well as on the sulfate balance of the systems. The complete quantification of in situ XRD measurements including the poorly crystalline C-S-H phase, as well as the meta-phyllosilicates gives a deeper insight into the behavior of the different phyllosilicates. This will further verify the mechanisms described previously and strengthen the understanding of complex blended cement systems using CC.

2. Materials and methods

2.1. Characterization of the meta-phyllosilicates

A detailed characterization of the meta-phyllosilicates (metakaolin (MK), metaillite (MI), metamuscovite (MM)) and descriptions of the methods used for characterization can be found in publications of clinker-free model systems [9, 15]. Table 1 summarizes the silicon (Si) and aluminum (Al) ion solubility and physical parameters as well as the zeta potential of the meta-phyllosilicates investigated in a synthetic model pore solution [16], Table 2 provides their chemical and mineralogical composition.

Table 1 Si- and Al-solubility of 1 g meta-phyllosilicate in 400 ml MOH solution, specific surface area, particle density, water absorption capacity and zeta potential of the meta-phyllosilicates investigated

	MK	MI	MM
Si [mmol l^{-1}]	7.97	3.44	0.44
Al [mmol l^{-1}]	7.64	1.85	0.29
Si/Al [-]	1.07	1.86	1.55
BET [m^2 g^{-1}] [17]	14.1	82.4	10.9
PD [g cm^{-3}] [18]	2.42	2.76	2.70
WAC [%] [19]	77.0	76.4	154.5
Zeta potential [mV] [16]	-47.3	-28.0	-9.5

Table 2 Chemical and mineralogical composition of meta-phyllosilicates investigated

Oxides (wt%)	MK	MI	MM	Phases (wt%)	MK	MI	MM
SiO_2	54.5	49.5	47.4	Quartz	5.0		
Al_2O_3	40.2	21.3	32.7	Anatase	0.6		
Fe_2O_3	1.8	6.6	5.1	Phengite	1.4		
CaO	< 0.1	6.9	0.2	Illite		31.3	
MgO	0.2	2.9	< 0.1	Calcite		3.6	
SO_3	< 0.1	< 0.1	< 0.1	Lime		0.5	
Na_2O	0.3	0.3	0.6	Portlandite		1.5	
K_2O	0.3	6.3	12.0	Muscovite			76.3
TiO_2	1.4	0.7	0.9				
LOI	1.3	5.4	0.9	X-ray amorphous	93.0	63.1	23.7

2.2. Synthetic cement (SyCEM) systems and test program

The synthetic cement (SyCEM) consists of synthetic monoclinic alite and cubic tricalcium aluminate C_3A. Bassanite and gypsum were used as sulfate carrier. The magnesium and aluminum stabilized M3 polymorph of alite was synthesized with a composition of 71.7 wt-% CaO, 25.9 wt-% SiO_2, 1.8 wt-% MgO and 0.6 wt-% Al_2O_3. The cubic C_3A was synthesized in the stoichiometric ratio of 3:1 ($3*CaO*Al_2O_3$). For the respective synthesis, the corresponding powders were homogenized in a vibrating disk mill using an agate tool, calcined at 1000 °C and then sintered in platinum crucibles in several sintering steps at 1400 °C for 5 or 6 hours. Between the individual sintering steps, the samples were crushed in the agate tool and finally ground to the required fineness. Bassanite was produced from gypsum (Merck) by dehydration at 85 °C for 7 days. Two reference systems were prepared, one pure system (SyCEM) and one with 10 wt-% of limestone powder (SyCEM-10LL). The limestone powder consists of 92 wt% calcite, 6 wt% dolomite and 2 wt% quartz with a BET of 6.0 m^2g^{-1} and a d_{50} of 20 µm. Its

characterization can be found in [20]. The composition of the reference systems and their specific surface areas (Blaine) are given in Table 3.

Table 3 Composition of the two reference systems in [wt-%] and their specific surface area (Blaine) in [m^2/g]

	Alite	C_3Acubic	Gypsum	Bassanite	LL	Blaine
SyCEM	87.25	8.5	3.5	0.75	-	≈ 4050
SyCEM-10LL	78.525	7.65	3.15	0.675	10	≈ 4100

The two reference systems were each substituted with 20 wt-%. of one of the three meta-phyllosilicates. The naming of the systems corresponds to their compositions, such as SyCEM-20MK or SyCEM-10LL-20MK. The w/b value for all tests is 0.6. In addition, sulfation of the accelerated meta-phyllosilicate systems was carried out. Gypsum was added for this purpose.

Isothermal calorimetry, in situ X-ray diffraction, thermogravimetry were performed. Before the start of each investigation, the materials were equilibrated overnight in a heating cabinet at measurement temperature (25 °C). The equilibrated samples were stirred manually with a spatula for 60 s and then immediately transferred to an appropriate crucible.

2.3. Particle size distribution

Particle size distribution (PSD) was performed on the three meta-phyllosilicates without and with ultrasonic treatment using the Bettersizer S3 plus from 3P Instruments. The stirrer was set to 900 rpm and then the sample was filled inside the instrument. After achieving optimum obscuration, the first measurement was carried out without ultrasound treatment. Subsequently, the sample was subjected to a 30 s ultrasonic treatment in the Bettersizer and then the PSD was measured again.

2.4. Isothermal calorimetry

Isothermal calorimetry experiments were performed with TA instruments TAM Air calorimeter at 25 °C for 50 h with 2 g of quartz sand in the reference chamber. The measured heat flow was normalized to 1 g of the SyCEM. Data analysis was done with Origin 2018b.

2.5. Thermogravimetry

Thermogravimetric (TG) investigations were carried out with Netzsch STA 449 F3. The samples were stopped with acetone after 6 and 48 h of hydration. The exact process for sample preparation and the experimental procedure is explained in [20]. The bound water was determined using the temperature interval from 20 to 400 °C and is referred to weight percent of the paste and normalized to 1 g of the SyCEM. The evaluation of the bound water is carried out in three temperature ranges from approximately 20-140°C, 140-190°C, and 190-400°C. The CH content was calculated from the mass loss in the temperature interval between 450 and 550 °C. The exact procedure and formulas for calculating the bound water and CH content are given in [9].

2.6. In situ X-ray diffraction

In situ XRD measurements were performed with a PANalytical Empyrean diffractometer equipped with a primary Bragg–BrentanoHD monochromator and a PIXcel^{1D} linear detector. A diffractogram was taken repeatedly in 15 min from 6 to 40° 2Θ at 40 kV and 40 mA with Cu Kα radiation for 50 h (200 scans). The sample holder of the diffractometer was connected to a temperature device that allowed in situ XRD measurements at the same temperature as the calorimetric measurements thus ensuring good comparability of both methods. The measurements were analyzed with High Score 4.7 [21] using Rietveld refinement [22, 23] with a combination of G-factor and PONKCS method [24, 25] according to Bergold et al. [26].

Table 4 lists all structures used for Rietveld refinement. In contrast to determining the phase content of the meta-phyllosilicates (section 2.1), the polycrystalline silicon disc was covered with Kapton film in order to calculate the factor G. For the application of the PONKCS method, hkl phase models were developed (Kapton film) and calibrated (free water, MK, MI, MM, calcium-silicate-hydrate (C-S-H)) for all non-crystalline components of the sample for which no structural data existed. The exact procedure is explained in [20] for creating the hkl-phase model of the Kapton film as well as for creating and calibrating the hkl-phase models of free water, MK and MM. The same procedure was applied to create and calibrate the hkl-phase model of MI. The C-S-H model was created according to Bergold et al. [26] and is described in detail in [9].

Table 4 Phases, Authors and ICSD numbers used for Rietveld refinement

Phase	Author	ICSD-No.
Silicon	[27]	52266
Alite	[28]	94742
C_3A_{cubic}	[29]	1841
Gypsum	[30]	92567
Calcite	[31]	40107
Illite	[32]	166963
Muscovite	[33]	68548
CH	[34]	34241
AFt	[35]	155395
AFm-Hc[1]	[36]	
Tobermorite[2]	[37]	403090
Kuzelite[3]	[38]	100138

[1]Hemicarboaluminatehydrate

[2]Structure information used for creating hkl-phase model for C-S-H

[3]Structure information used to quantify Calcium Aluminum Sulfate Hydrate ($Ca_4Al_2O_6(SO_4)$ x 14 H_2O PDF-Nr: 42-0062 [39], abbreviation:$C_4A\$$ x H_{14})

In order to ensure stable refinement over the measurement period of 200 scans, as few parameters as possible should be unlocked during Rietveld refinement, especially if the

PONKCS method is used with several hkl-phase models. The lattice parameter of the SyCEM phases alite, C_3A_{cubic}, gypsum and calcite were refined on pure powder samples and kept fixed during refinement of the paste. A schematic illustration of the analysis routine is given in [9]. For MI and MM, both the scaling factor of the hkl-phase models and the crystalline structure were refined and presented as a sum.

The degree of hydration (DoH) of alite or degree of reaction (DoR) of the meta-phyllosilicates was calculated from the respective initial values and the data from in situ quantification, smoothed by a fast fourier transformation (FFT) filter. The calculation of CH consumption and C-S-H formation is based on the difference between the quantified content and the content calculated from the reacted alite according to equation 1.

$C_3S + 3.9\ H \rightarrow C_{1.7}SH_{2.6} + 1.3\ CH$ (equation 1)

The reaction rate of AFt was calculated using the content of AFt right at the beginning of hydration (AFt start), the content of AFt at the onset of accelerated AFt formation (AFt at onset), and the time interval until the onset of accelerated AFt formation (Time until AFt onset) according to the following equation.

$$Reaction\ Rate\ (AFt)[wt\%\ h^{-1}] = \frac{AFt\ at\ onset\ [wt\%] - AFt\ start\ [wt\%]}{Time\ until\ AFt\ onset\ [h]}$$

3. Results and discussion

3.1. Particle size distribution

The PSD without and after 30 s ultrasound treatment (a) and their differences in PSD (b) is shown in Figure 1. The results yields clear differences between the individual meta-phyllosilicates. For MM, the ultrasound treatment leads only to small differences of 1 - 2 Vol.-% at the peak. MI and MK, on the other hand reveal very significant differences and thus a clear refinement of the PSD by ultrasound treatment. These results indicate the extent to which the different meta-phyllosilicates agglomerate. MM hardly agglomerate while MI and MK clearly agglomerate with maxima at 60 µm and 40 µm respectively. Table 5 summarizes the d_{10}, d_{50} and d_{90} values before and after ultrasound treatment.

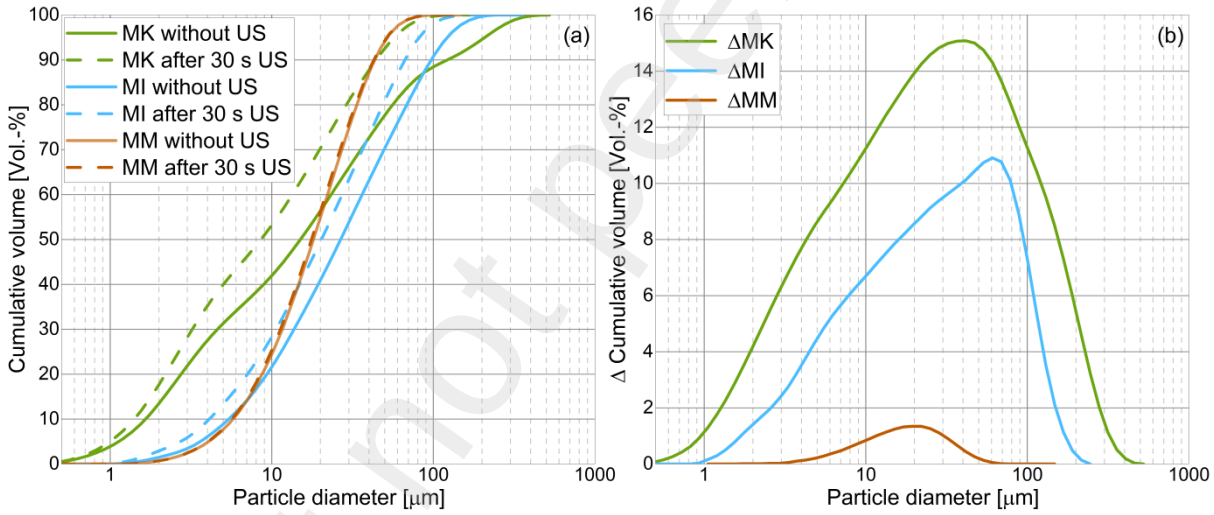

Figure 1 PSD before and after ultrasound (US) treatment (a) and their differences (b)

Table 5 Summary of the results of the PSD before and after ultrasound treatment

	MK		MI		MM	
	Before US	After US	Before US	After US	Before US	After US
d_{10} [µm]	1.7	1.4	5.4	4.1	5.8	5.7
d_{50} [µm]	15.0	8.6	26.7	20.3	18.1	17.6
d_{90} [µm]	122.0	44.1	96.6	66.4	43.1	42.6

3.2. Isothermal calorimetry

The heat flow of SyCEM with 20MK replacement and different sulfation (Figure 2a) shows a similar influence on the silicate reaction at all sulfation levels. Only a minor difference to the reference system can be observed. With limestone powder, all sulfation levels also behave synchronously with respect to the silicate reaction. Here, the addition of 20MK leads to an acceleration of the silicate reaction compared to SyCEM-10LL (Figure 2b). The influence of 20MK on the aluminate reaction is identical with and without limestone powder. While the differences between the maximum of the silicate and the aluminate reaction in the reference systems are > 15 h, the addition of 20MK leads to a strong acceleration of the aluminate reaction and thus to a decrease of the difference to < 3 h. The low sulfate contents result from dilution of the reference systems with 20 wt-% meta-phyllosilicate. Adding more gypsum results in a comparable retardation of the aluminate reaction with and without limestone powder for both sulfation levels. The sulfation corresponding to the original sulfate content of the reference systems (2.0 and 1.8 % SO_3) is not sufficient to reestablish the difference between silicate and aluminate reactions. Finally, a further increase of the sulfate content by 50 % leads to a retardation of the aluminate reaction beyond the level of the reference systems.

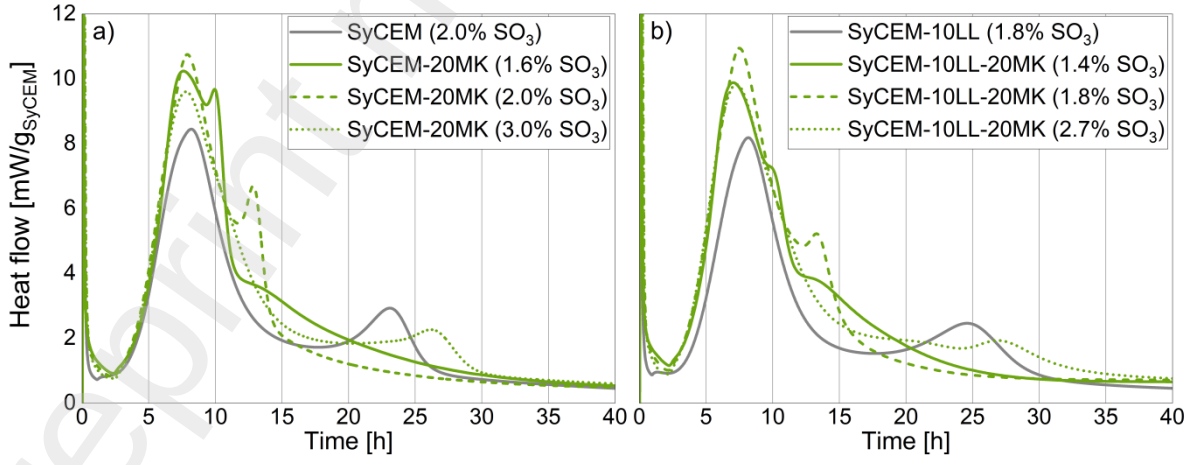

Figure 2 Heat flow with 20MK replacement and different sulfation of SyCEM (a) and SyCEM-10LL (b) systems

The calorimetric investigations of the 2:1 phyllosilicates MI and MM (Figure 3) yield a less pronounced acceleration of the aluminate clinker reaction compared to the MK systems. The difference between the maximum of the silicate and aluminate clinker reaction is 5 - 6 h. In case of the systems with MM a sulfation of 2.0 and 1.8 % resp. is already sufficient to reestablish the initial condition of the reference system. The retardation of the aluminate reaction in the systems with MI lies between MK and MM. The sulfation of 2.0 and 1.8 % is almost sufficient to reach the condition of the reference system. The silicate reaction is accelerated compared to the reference both with and without limestone powder for the SyCEM – 20MM systems and with limestone powder only for the SyCEM - 20MI systems. The influence on the silicate clinker reaction is comparable for MK and MI and differs from the influence on MM. Since the meta-phyllosilicates exhibit significant differences in their PSD and BET, no direct correlation of the physical filler effect and the PSD or BET of the meta-phyllosilicates can be established. Maier et al. [10] justify this observation based on a comparison between limestone powder and kaolinite-rich clays with an agglomeration of clay minerals compared to limestone powder. MM is not prone to such agglomeration (see Figure 1) and can thus exploit the physical influence of the silicate reaction by the filler effect and the available surfaces for nucleation of the C-S-H phases.

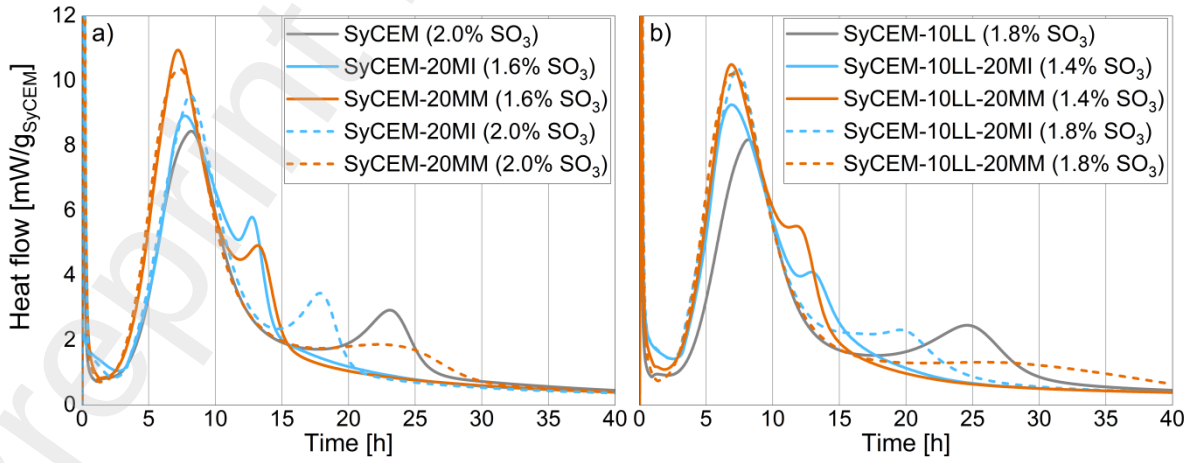

Figure 3 Heat flow with 20MI or 20MM replacement and different sulfation of SyCEM (a) and SyCEM-10LL (b) systems

3.3. Thermogravimetry

The results of the TG measurements are presented in Figure 4. After 6 hours, the CH content differs hardly (Figure 4a and b). The systems with MM show slightly higher CH contents than the reference systems, which is in line with the stronger acceleration of the silicate reaction. The influence of the meta-phyllosilicates becomes clear after 2 days. Both without and with LL, the systems with MK and MI have lower CH contents than the reference, indicating the chemical reactivity of the meta-phyllosilicates. The MM systems are in the range of the reference after 2 d or reach a slightly higher value than the reference systems. Thus, no portlandite consumption and therefore no chemical reactivity of the MM is detectable.

The sum of bound water is higher for all meta-phyllosilicates than for the corresponding reference systems (Figure 4c and d). This can be attributed to the accelerated alite hydration of the MM systems, and to the chemical reactivity of the phyllosilicates for MK and MI. In addition, for MK an increased water binding is visible in “Stage 2”. This corresponds to earlier observations [40] and is attributed to the higher content of reactive aluminum in MK compared to 2:1 phyllosilicates.

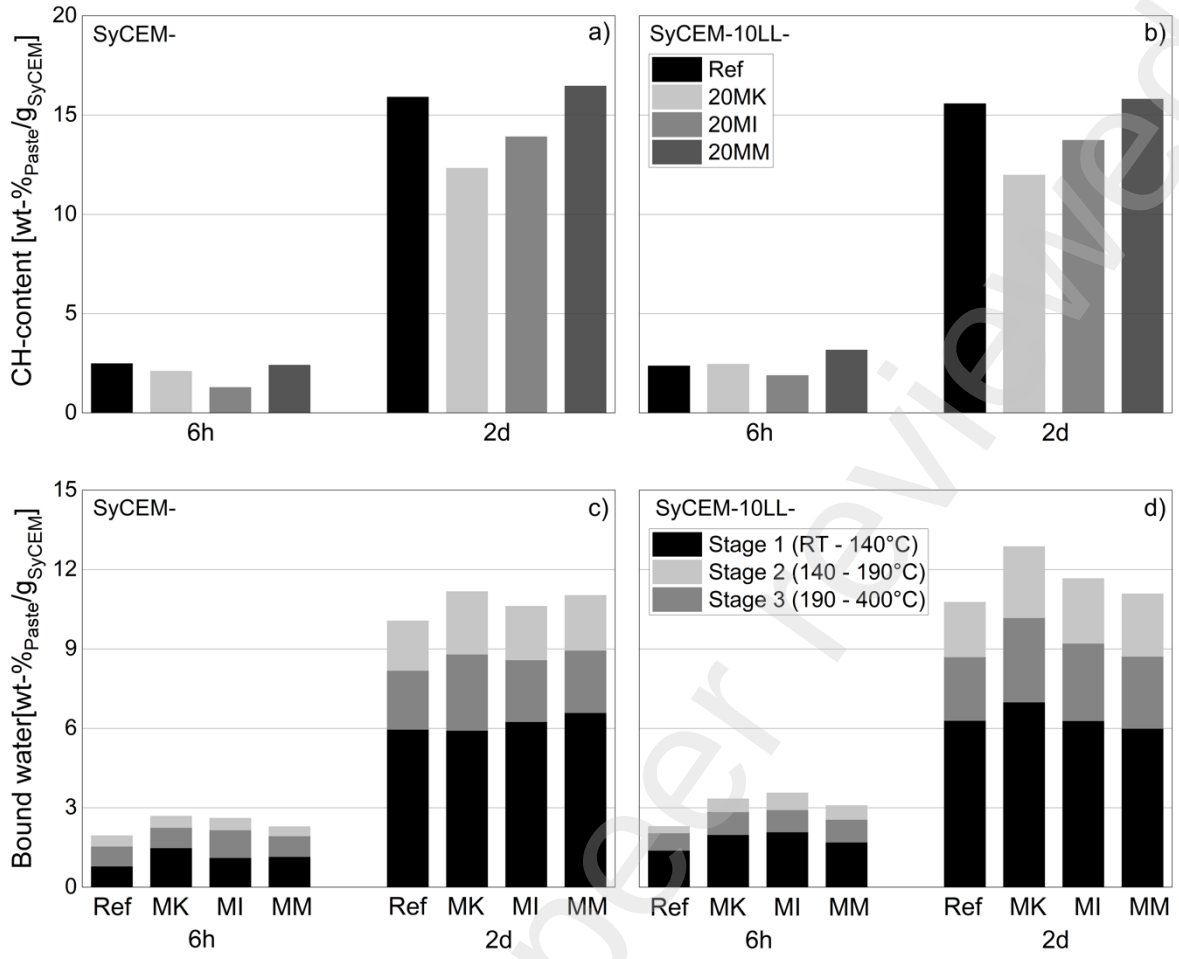

Figure 4 CH-content (a and b) and bound water (c and d) after 6 h and 2 d. The values are normalized to wt-% of the paste per gram of the synthetic cement (SyCEM).

3.4. In situ X-ray diffraction

0 shows the quantification of the reference systems (a and b) and the 20MK systems (c and d). Alite hydration progresses comparably for both reference systems. The onset of alite hydration after 4-5 hours is accompanied by the first formation of CH. Quantification of C-S-H is possible 2-3 hours after the onset of alite hydration. This is due to the small crystallite size of the C-S-H at the beginning of alite hydration, as shown by Bergold et al. [26]. With replacement of 20MK, alite hydration appears to be slightly accelerated but less pronounced compared to the reference systems.

The aluminate reaction goes along with an initial dissolution of bassanite, gypsum and C_3A, and initial formation of AFt between 0.7 and 1.7 wt-% (Table 7) after the first scan of the in situ XRD analysis (15 minutes). This is followed by continuous AFt formation until complete dissolution of the gypsum and subsequent accelerated AFt formation until it reaches its maximum content (AFt_{max}). Subsequently, the reaction in the limestone-free systems continues to form monosulfate hydrate (AFm-MS) at the expense of Aft while the addition of LL stabilizes AFt and its reaction to hemicarboaluminate hydrate (AFm-Hc), as already known from other studies [41, 42] and thermodynamic modeling [43]. Overall, the MK addition accelerates significantly the aluminate reaction. This is evidenced by the significantly earlier occurrence of AFT_{max} and higher contents of AFm-MS and AFm-Hc after 50 h compared to the respective reference system.

The decrease in MK content indicates a continuous reaction contribution of MK during early hydration. There exist only minor differences between the MK systems without and with LL and the content after 50 h declines to 6% for both systems due to its dissolution [44].

Figure 6 shows the quantification of the 20MI systems (a and c) and the 20MM systems (b and d). Adding 20MM accelerates the silicate reaction (onset of Alite hydration after 3-4 h) and significantly more alite reacts during the first 15 hours, which confirms the observations of the calorimetry measurements and indicates a better filler effect of the MM in comparison to MK and MI and less agglomeration of the MM particles. Analogous to the reference systems, the first CH formation occurs parallel to alite reaction, while the C-S-H is only quantifiable several hours later.

Both, 20MI and 20MM strongly accelerate the aluminate reaction compared to the reference, but to a lesser extent than in the 20MK systems. AFt_{max} is reached after 12 – 14 h for all four

systems. The contents of AFm-Ms and AFm-Hc are similar for MI and MM, but significantly below those of the 20MK systems.

The results indicate a higher chemical reaction contribution in the case of MK as observed in clinker free model systems [9], due to the higher absolute solubility of aluminum and the lower Si/Al ratio compared to the 2:1 phyllosilicates MI and MM. This is evidenced by the quantification of the MI and MM. The MM content is not provided, since no decrease can be determined during the first 50 hours and thus no chemical reaction contribution of the MM takes place. MI exhibits a very slow but continuous decrease and thus reaction contribution, which is significantly lower compared to MK.

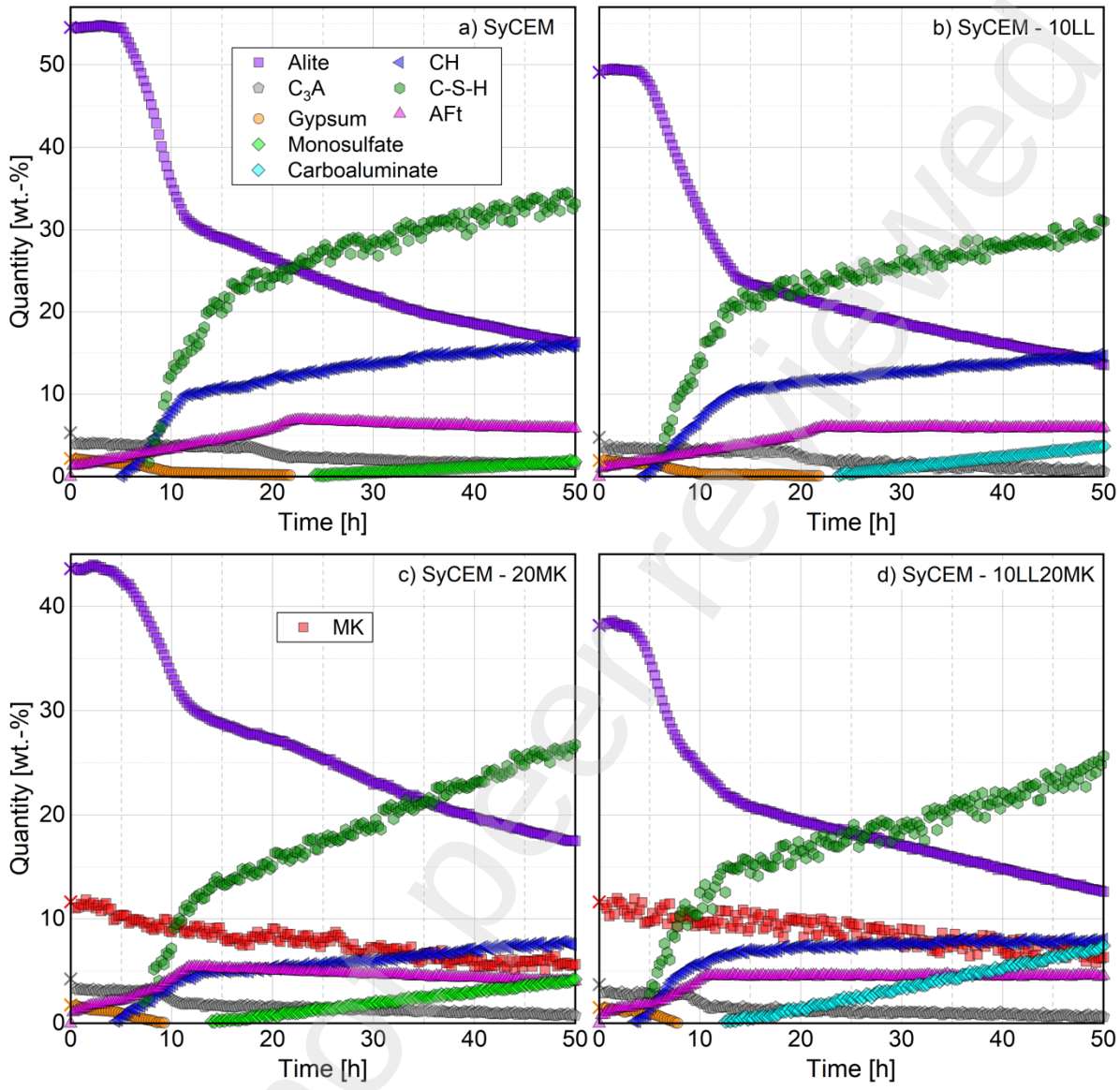

291

292

293 **Figure 5** Quantification of in situ XRD measurements of the reference systems (a and b) and

294 of the SyCEM - 20MK systems (c and d)

295

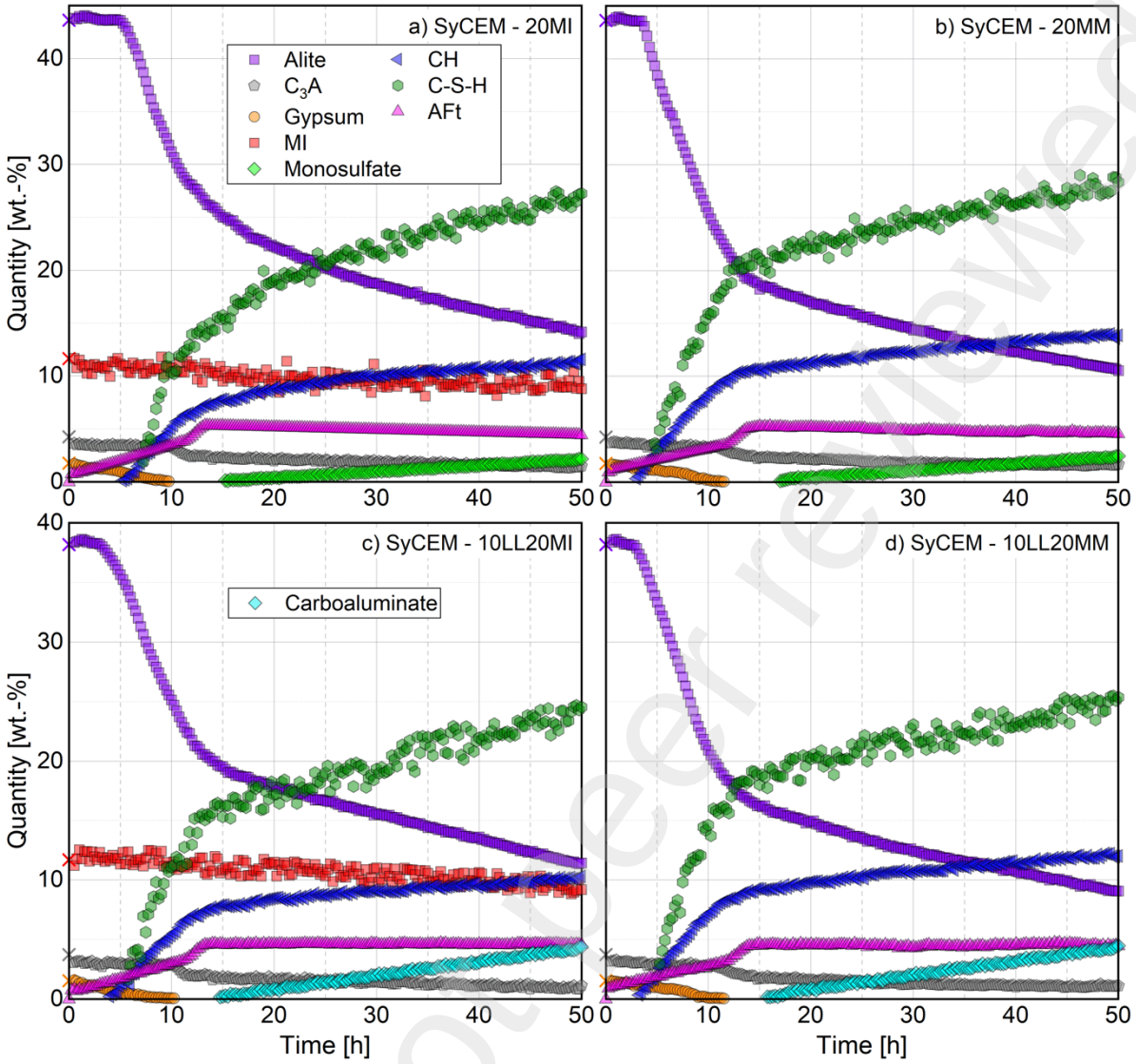

Figure 6 Quantification of in situ XRD measurements of the SyCEM - 20MI systems (a and c) and of the SyCEM - 20MM systems (b and d)

Figure 7 shows the quantification of the highly sulfated 20MK systems, which shifts the aluminate reaction to such an extent that it becomes similar to the reference system (dotted line in Figure 2). Compared to the 20MK systems with low sulfate content (0c and d), no difference is observed at the onset of Alit hydration. It is obvious especially for the systems without LL that significantly more alite reacts during the first 15 hours. The onset of accelerated AFt formation occurs after about 22 hours for both systems and is thus clearly shifted to a later point in time. In the time interval until accelerated AFt formation starts, more AFt is formed compared to the lower sulfated systems (0). As a result of the shift of the aluminate clinker

reaction, the formation of AFm-Ms or AFm-Hc occurs later and reaches a lower content after 50 h compared to the undersulfated 20MK systems. The quantification of MK does not differ between the low and highly sulfated systems within the error margin.

Overall, it is confirmed that the additional sulfate addition strongly affects the aluminate as well as the silicate clinker reaction.

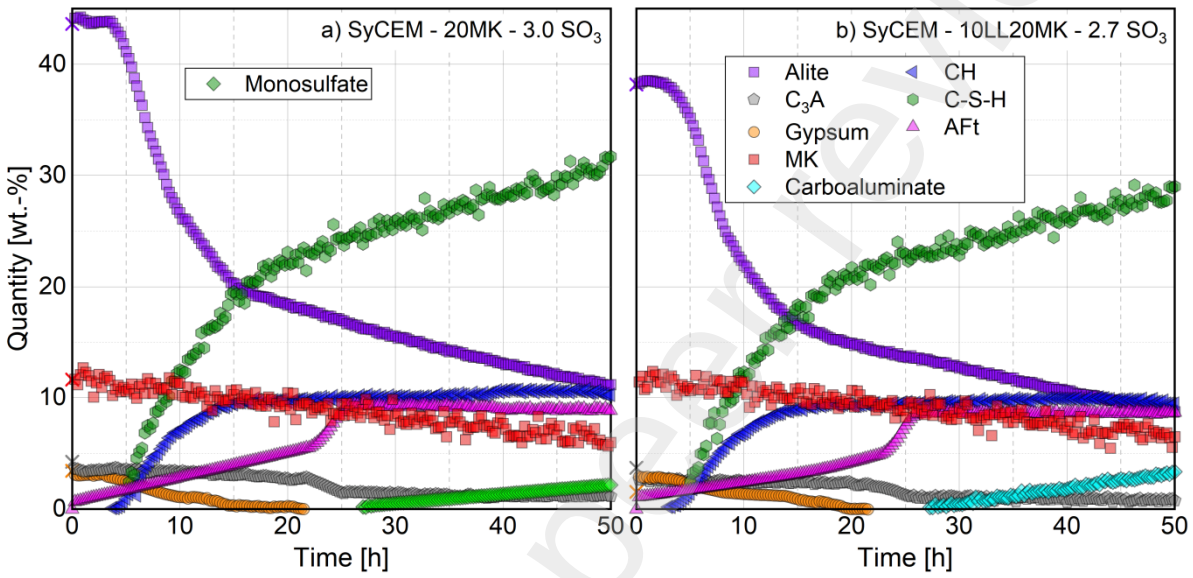

Figure 7 Quantification of in situ XRD of the sulfated SyCEM - 20MK systems (dotted lines in Figure 2)

3.5. Implications regarding the interaction of meta-phyllosilicates with the silicate reaction

The calculation of the DoH of Alite from the XRD quantifications in Figure 8 clearly illustrates the different influence on the silicate clinker reaction by the individual meta-phyllosilicates. First, the comparison of the reference systems shows that the interaction of LL leads to a slight increase of the DoH of alite. The influence of limestone powder on early hydration is largely determined by its fineness [45]. A higher fineness leads to a stronger acceleration and thus to a higher DoH of alite compared to the reference system without LL replacement [10, 45]. The fineness of the LL used is in the range of the clinker phases (see Blaine values of the SyCEM

systems in Table 3), which means that this is not causing the acceleration of alite hydration here. However, the higher DoH of alite for the SyCEM-10LL system can be attributed to the additional dilution of the system and thus more space for the formation of hydrate phases and the filler effect of LL, which promotes the hydration of alite. This is confirmed when considering the systems containing meta-phyllosilicates, which show an increase of the DoH of alite in systems with LL. Compared to the reference systems, only the 20MM systems yield a higher DoH, while using 20MK or 20MI decreases in the DoH of alite. For their part, the meta-phyllosilicates show a gradation of the DoH of alite from MM with the highest, to MI and finally MK with the lowest DoH of alite. The strong decrease of the DoH of alite for the 20MK system is remarkable. Also in the 10LL20MK system, alite has a lower DoH compared to the reference. However, the addition of the limestone powder causes a lower decrease of the DoH of alite. Maier et al. [10] also report a decrease of the DoH of alite when using a calcined kaolinite-rich clay with a kaolinite content of 69 wt.%. They describe an accelerated alite hydration and an increase of the DoH of alite with the limestone powder used. The authors partly attribute this to the different behavior of LL and calcined clay particles. While LL provides a larger part of its surface for nucleation and growth of C-S-H phases, calcined clay particles tend to agglomerate. This leads to a significantly less pronounced filler effect than expected from the BET surface area and PSD of calcined clay particles. A second explanation provided is a different surface charge of the particles and an associated adsorption of Ca^{2+} and SO_4^{2-} ions on the surfaces of the clay particles. The comparison of the zeta potentials of the meta-phyllosilicates delivers the most negative value for MK (Table 1), which can be regarded as the reason for the strongest interference regarding the ion balance of the pore solution. MI, on the other hand, causes a lower impediment of alite hydration, while for MM with the lowest zeta potential of -9.5 mV no impediment of alite hydration is detectable. On the contrary, the addition of MM has a strong filler effect comparable to fine limestone powder [45]. The

differences between the systems become even more apparent when the DoH of alite at the time of onset of accelerated AFt formation is examined (Table 8). While the MM systems reach the DoH of the reference systems, a significant drop in the DoH of the Alit can be observed for the MI and MK systems. This is another indication that the surfaces of the calcined clay particles influence the sulfate balance.

The additional dosage of sulfate to the 20MK systems leads to a significant increase of the DoH of alite compared to the low sulfate 20MK systems. This confirms the observations of [10, 46] that the timing of accelerated C_3A dissolution and accelerated AFt formation significantly affects the DOH of alite.

The clear shift of the aluminate reaction of the 20MI and 20MM systems already at a low addition of sulfate (dashed lines in Figure 3) also indicate a lower influence by adsorption effects of the 2:1 meta-phyllosilicates MI and MM compared to the 1:1 meta-phyllosilicate MK. It can be assumed that an additional sulfate addition to the 20MI systems would cause a slight increase of the DoH of alite, while the 20MM systems already reach a very high DoH in the low sulfated systems and thus do not require any further sulfate carriers from the perspective of the DoH of alite.

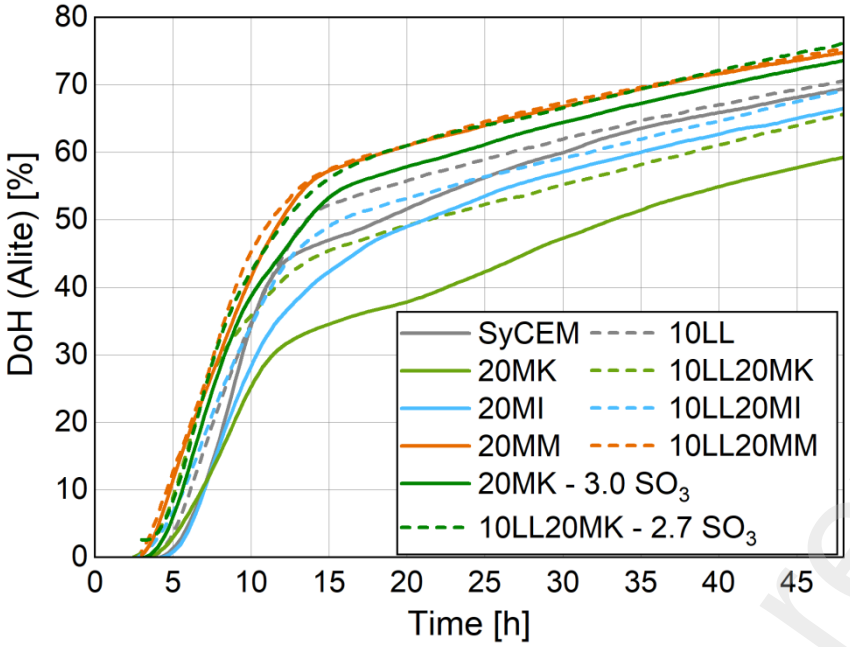

Figure 8 Degree of hydration (DoH) of Alite calculated from the XRD quantifications

3.6. Implications regarding the influence of meta-phyllosilicates on the sulfate balance

Even though the addition of meta-phyllosilicates accelerates the silicate reaction and thus leads to an earlier onset of alite hydration as described before [10, 47, 48], this does not result in a higher DoH of alite for MK and MI systems after completion of the main reaction. Figure 9 shows the DoH of alite at the onset of the aluminate reaction depending on the difference of the total sulfate content and the bound sulfate content in AFt analogous to [10]. After [49, 50], the added sulfate carrier is completely dissolved at the onset of the aluminate reaction which is also the case in this study (0 - Figure 7). Thus, the sulfate that is not bound in AFt must be present in the pore solution or adsorbed on available surfaces. The data points of the two model cement systems SyCEM and SyCEM-10LL are close to each other (Figure 9), indicating only slight differences of the silicate and aluminate reaction. The PSD of the LL leads only to a slight filler effect and thus to a slight increase of the DoH of alite. The MM systems also show only small differences of the DoH of alite to their reference systems. The slight shift along the x-axis

indicates a somewhat lower AFt content, which can be explained by the significant acceleration of the aluminate clinker reaction and thus less time for AFt formation. Zunino and Scrivener [51] describe a correlation between the quantity of C-S-H phases formed and the acceleration of the aluminate clinker reaction due to the adsorption of sulfate on the C-S-H surfaces during their formation. For MM systems, the formation of the C-S-H and thus the DoH of alite can also be considered as the driving force for the acceleration of the aluminate reaction. The influence of MM on early clinker hydration is comparable to the influence of LL and, according to [45], depends essentially on the fineness of the particles: a higher fineness increases the DoH of alite.

More differences exist for the MI systems, although the acceleration of the aluminate reaction is comparable for the MI and MM systems, respectively (see Figure 3). The DoH of alite is lower at the onset of the aluminate reaction in case of MI systems and significantly lower in case of MK systems. These observations are consistent with the observations of Maier et al. [10] who conclude that the meta-clay surfaces serve as host for the adsorption of sulfate in addition to C-S-H. The results in Figure 9 confirm this assumption. The adsorption of sulfate in the case of MI and MK cannot be attributed to the ongoing formation of C-S-H alone. In fact, the results illustrated in Figure 9 confirm the adsorption effects of calcium – sulfate complexes as reported by [5, 10] on the meta-phyllosilicate particle surfaces. This is consistent with the increasing negative zeta potential of the meta-phyllosilicates from MM over MI to MK (Table 1, [16]) and in line with observations in systems with two kaolinitic clays with different zeta potentials [10]. A direct link to the BET surface or to the PSD (Table 1) cannot be established in the comparison of different meta-phyllosilicates.

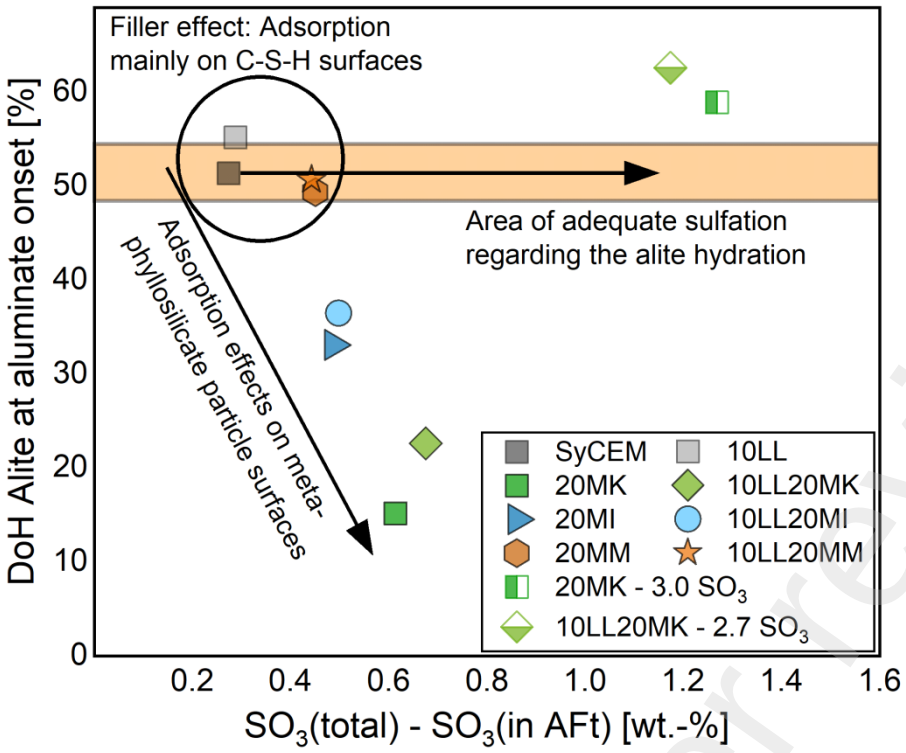

404

405 **Figure 9** Correlation of the SO_3 content with the DoH of Alite at the onset of accelerated AFt
406 formation (Table 8). The SO_3 content is calculated from the difference between the total
407 SO_3 content and the SO_3 bound in AFt analogous to [10].

408 The orange band in Figure 9 indicates the area of adequate sulfation based on the DoH of alite.
409 The highly sulfated MK systems (half-filled points in Figure 9), indicate a higher DoH of Alite.
410 The time shift of the aluminate clinker reaction (Figure 2) leads to an unimpeded alite hydration
411 and a higher DoH of alite at the aluminate onset compared to the respective reference systems.
412 Thus, for the present MK systems, adequate sulfation according the orange area can already be
413 achieved with lower sulfate dosages. The higher amount of adsorbed sulfate (shift along the x-
414 axis) does not seem to influence alite hydration in the case of a retarded aluminate clinker
415 reaction.

416 The mechanisms behind the impediment of alite hydration remain unclear. It is known that
417 aluminum, alkali and sulfate have a great influence on alite hydration [52, 53]. While the
418 presence of sulfate has a positive influence on the DoH of the alite [53], the presence of

aluminum in the pore solution leads to an impediment of alite hydration [54]. In addition to the cement phases, another phase, the meta-phyllosilicates, could compete for the sulfate by adsorbing sulfate on their surfaces and thus hinder alite hydration. The high content of adsorbed sulfate and the rapid conversion to AFt in the highly sulfated systems support the conjecture of Maier et al. [8] that adsorbed ions are more readily desorbed on the meta-phyllosilicate surfaces than on C-S-H surfaces. Furthermore, Jansen et al. [14] show with their complete mass balance approach that the aluminum concentration in the pore solution increases significantly at the onset of accelerated AFt formation, but no aluminum can be detected in the pore solution up to this point. The authors assume that the aluminum already dissolved from the cement phases is adsorbed on surfaces or attributed to an aluminum enriched layer of C_3A as stated by Myers et al. [5]. The influence of additional aluminum from the meta-phyllosilicates on the mass balance and pore solution could lead to an impediment of alite hydration.

3.7. Implications regarding the reactivity of the meta-phyllosilicates

Table 6 lists the DoR of the meta-phyllosilicates based on the value of the FFT fit after 50 h. Although the DoR from the XRD quantification has a large error [44] clear trends can be identified that are consistent with the observations from the clinker-free systems [9]. The DoR of the MK is around 48 ± 3 % for all MK systems and in the range reported by [55]. Thus, no differences in the DoR of the MK can be seen from the XRD quantification, neither by using LL nor by additional sulfate doses. Also for MI and MM the addition of LL has no impact on the DoR of the 2:1 meta-phyllosilicates. MI with a DoR of 20 % reaches about 40 % of the reactivity of MK. No reactivity is detectable for MM during the first 50 h, as already mentioned in section 3.4. The overall trend of the reactivity of the meta-phyllosilicates is in line with the reactivity observed in clinker-free model systems [9].

Table 6 Degree of reaction (DoR) of the meta-phyllosilicates calculated based on the value after 50 h of the FFT fit of the in situ XRD quantifications

	20MK	20MK - 3.0 SO_3	10LL 20MK	10LL 20MK - 2.7 SO_3	20MI	10LL 20MI	20MM	10LL 20MM
DoR meta-phyllo-silicate	51	48	46	45	20	22	3	3

A part of the chemical reactivity of the meta-phyllosilicates can be illustrated by the time course of the CH consumption during the first 50 h (Figure 10). The calculation is based on the alite hydration and equation 1. In addition, the value calculated from TG analysis after 48 h is plotted. Figure 10 confirms again that MM does not show a pozzolanic reaction during early hydration and thus does not consume CH. The course is almost identical to the reference. The underestimation at the beginning of alite hydration can be explained by the very high hydration rate of alite and the low resolution of the in situ XRD analyses of 15 minutes. For the 20MI and 20MK systems, a difference in the course of CH consumption is noticeable. Whereas in the case of MI, CH consumption is evident from about 20 h, in the case of the highly sulfated MK and the 10LL20MK systems, CH consumption starts after about 15 h. Only the 20MK system shows an even earlier CH consumption after about 10 h. Overall, the 20MK consumes more CH especially between 10 and 20 h, which could indicate an increased activity of the MK during this period which might influence the hydration of the clinker phases. However, the time course of the XRD quantification of the MK (0c) cannot validly confirm a higher reactivity between 10 and 20 h. After 50 h, the CH consumption of all investigated 20MK systems is in a close range (see Table 8) analogous to the calculation of the DoR of MK. The general trends of the evaluation of the reactivity of the meta-phyllosilicates based on the CH consumption after 50 h

462 hours and after 48 h from the TG analysis, respectively, confirm the previous observations: MM
463 shows no, MI a medium and MK the highest reactivity.

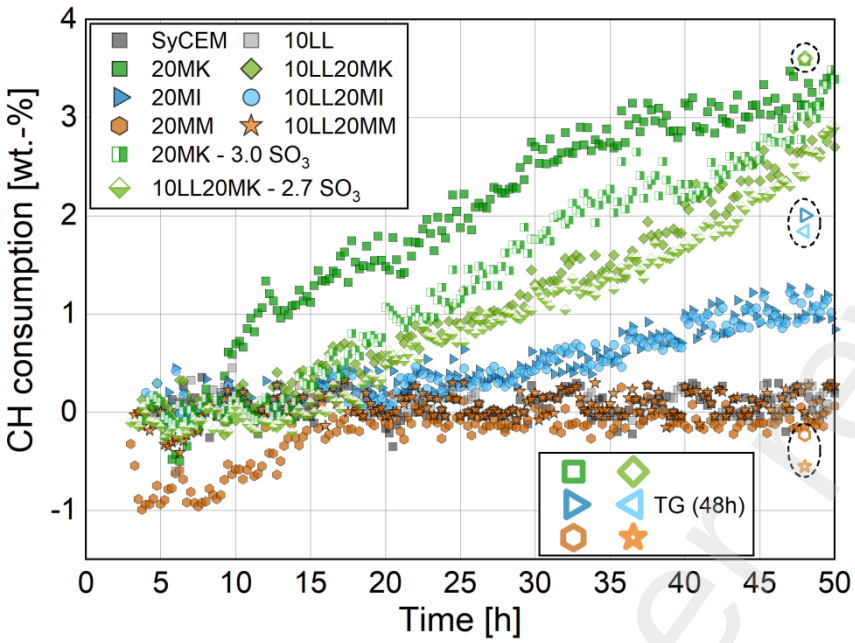

464

465 **Figure 10** CH consumption of all systems quantified based on alite hydration and
466 equation 1 (section 2.6). In addition, the value calculated from TG analysis after 48 h is
467 plotted.

468 The calculation of C-S-H formation (Figure 11) based on alite hydration and equation 1 yield
469 the same trends. The C-S-H formation after 50 h (50 h value of the FFT fit Table 8) is
470 underdetermined by about 2 wt.-% for the SyCEM and the 20MM systems. This under-
471 determination can consequently also be assumed for 20MI and 20MK systems, where the C-
472 S-H formation takes on slightly negative values (20MI) and positive values between 1.5 and
473 2.6 % (20MK). The increasing trend for the MK and MI systems represents the C-S-H formed
474 through pozzolanic reaction and verify a chemical reaction contribution of MK and MI.

475

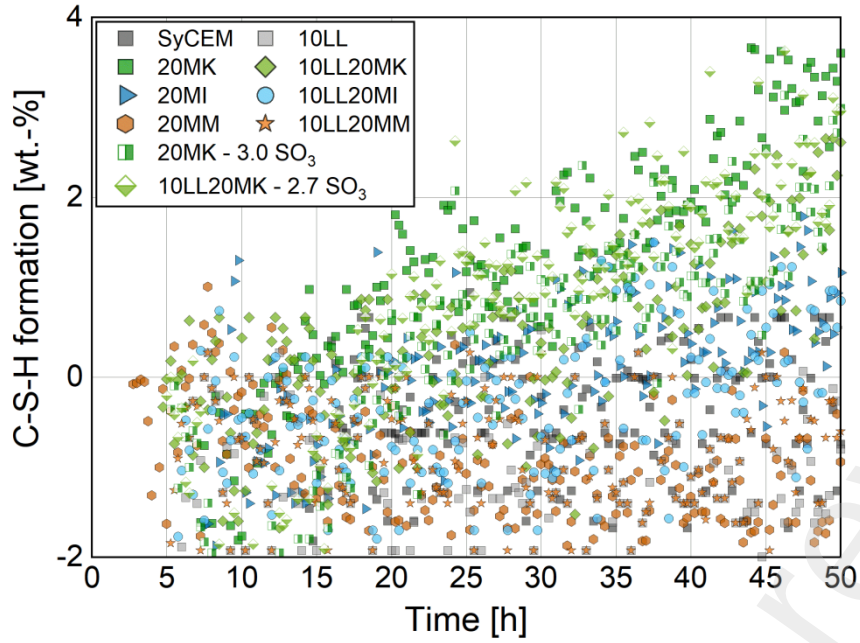

476

477 **Figure 11** C-S-H formation of all systems quantified based on alite hydration and
478 equation 1 (section 2.6)

479 The influence of the reactive aluminum of the meta-phyllosilicates is much more difficult to
480 identify. The very high initial dissolution of the C_3A means that sufficient aluminum is available
481 for the formation of AFt already at the beginning of the hydration. Table 7 summarizes the key
482 data concerning the formation of AFt. Within the error of quantifying the hydrating systems,
483 the differences must be considered as small. The initial formation of AFt (AFt Start) right at the
484 beginning of the hydration shows lower values for the meta-phyllosilicate systems compared to
485 the respective reference systems. Lower AFt contents are also observed at the onset of
486 accelerated AFt formation, with the most reactive meta-phyllosilicate MK surprisingly showing
487 the lowest AFt content (AFt at onset). Thus, no direct influence of the reactive aluminum by
488 higher AFt contents can be demonstrated. However, considering the reaction rate of the AFt
489 (equation 2, section 2.6) until the onset of the accelerated AFt formation, slightly increased
490 values are found for the MK and MI systems compared to the respective reference and MM
491 systems. The extent to which an increased AFt formation rate can be explained by interaction

with the sulfate carrier through adsorption effects (Figure 9) or the reactivity of the meta-phyllosilicates (Table 6) remains open at this point.

Table 7 Summary of the key data concerning the formation of AFt

	SyCEM	20MK	20MI	20MM	20MK - 3.0 SO3
Time onset AFt [h]	19.75	8.50	11.00	11.75	22.00
AFt Start [wt-%]	1.68	1.09	1.02	1.15	0.79
AFt at onset [wt-%]	5.77	3.33	3.74	3.86	5.52
Reaction rate [wt-%/h]	0.21	0.26	0.25	0.23	0.22
	SyCEM-10LL	10LL20MK	10LL20MI	10LL20MM	10LL20MK – 2.7 SO3
Time onset Aft [h]	19.50	6.75	9.50	11.50	21.50
Aft Start [wt-%]	1.34	0.90	0.96	0.91	0.68
AFt at onset [wt-%]	5.06	2.46	3.04	3.22	4.86
Reaction rate [wt-%/h]	0.19	0.23	0.22	0.20	0.19

Overall, the present investigation does not proof a direct influence of the reactivity of the meta-phyllosilicates on the silicate clinker reaction and on the aluminate clinker reaction. Nevertheless, an influence on the sulfate balance by the reaction contribution of aluminum from the meta-phyllosilicates can be assumed, especially on the sulfation of the systems. Meta-phyllosilicates with a higher reactivity cause a shorter time shift of the aluminate clinker reaction and thus a higher sulfate demand.

4. Conclusion

The present study clearly shows that such significant differences occur not only between limestone powder and calcined kaolinite-rich clays, but do already exist between individual meta-phyllosilicates The investigation of three different meta-phyllosilicates metakaolin (MK), metaillite (MI) and metamuscovite (MM) in model cement systems lead to the following conclusions:

- MM acts solely as filler without chemical reactivity during early hydration and accelerates the early alite hydration.
- MK and MI accelerate the aluminate clinker reaction in all model systems and decrease the DoH of alite. The extent to which the negatively charged surface of the meta-phyllosilicate particles influences the hydration of alite and C_3Athrough adsorption and desorption effects of calcium - sulfate complexes is still not clear.
- Due to agglomeration especially of MI and MK particles, no correlation of their influence on early hydration to PSD and BET surface area can be established for all three meta-phyllosilicates.
- MK and MI show a clear chemical reactivity already during the first day of hydration, which can be determined directly by the quantification of meta-phyllosilicates as well as indirectly by the consumption of portlandite and increased contents of C-S-H.
- The extent to which the chemical reactivity of the meta-phyllosilicates has an influence on the reaction kinetics and sulfation of the systems cannot be finally clarified.
- The investigations in the model cement systems confirm the reactivity of the individual meta-phyllosilicates experienced in the clinker-free model systems [9]. In the present investigations, the reactivity of MI is about 40% of MK, while MM exhibits no measurable reactivity during the first two days.

5. Acknowledgement

The authors like to thank Deutsche Forschungsgemeinschaft (DFG) for the financial support of the research project “Efficiency and influence of calcined phyllosilicates during the early hydration of cement” (BE 7038/2-1).

6. Appendix

Table 8 Summary of the values from the XRD quantification after 50 h (FFT5 - fit)

	DoH Alite at AFt onset	DoH Alite	CH consumption	C-S-H formation
SyCEM	51.5	70.2	-	-2.0
SyCEM10LL	55.2	72.4	-	-2.4
SyCEM20MK	15.2	59.9	3.5	2.6
SyCEM20MK - 3.0 SO_3	59.0	74.3	3.8	1.9
SyCEM10LL20MK	22.7	66.9	2.7	1.5
SyCEM10LL20MK – 2.7 SO_3	61.7	77.0	2.9	2.3
SyCEM20MI	33.1	67.5	0.8	-0,66
SyCEM10LL20MI	32.0	70.0	1.0	-0.2
SyCEM20MM	49.5	75.8	0	-2,2
SyCEM10LL20MM	50.7	76.4	0.3	-1.7

7. References

1. K. Scrivener, F. Martirena, S. Bishnoi, and S. Maity, *Calcined clay limestone cements (LC³).* Cement and Concrete Research. 114 (2018) 49-56. https://doi.org/10.1016/j.cemconres.2017.08.017

2. R. Sposito, M. Maier, G. Cordoba, S. Scherb, A. Tironi, N. Beuntner, A. Neißer-Deiters, E. F. Irassar, and K.-C. Thienel, *Transferability from Pure Metaphases to Calcined Common Clays – New Insights into Particle Properties and Prediction Models*, in *International Conference on Calcined Clays for Sustainable Concrete*, M. Sharma, H. Hafez, F. Zunino, and K. Scrivener, Editors. (2022): Lausanne, Switzerland. p. 110-111.

3. R. Sposito, M. Maier, N. Beuntner, and K.-C. Thienel, *Physical and mineralogical properties of calcined common clays as SCM and their impact on flow resistance and demand for superplasticizer.* Cement and Concrete Research. 154 (2022) 106743. https://doi.org/10.1016/j.cemconres.2022.106743

4. A. Favier, C. De Wolf, K. Scrivener, and G. Habert, *A sustainable future for the European Cement and Concrete Industry. Technology assessment for full decarbonisation of the industry by 2050*. (2018), ETH Zurich.DOI: https://doi.org/10.3929/ethz-b-000301843.

5. R. J. Myers, G. Geng, J. Li, E. D. Rodríguez, J. Ha, P. Kidkhunthod, G. Sposito, L. N. Lammers, A. P. Kirchheim, and P. J. M. Monteiro, *Role of Adsorption Phenomena in Cubic Tricalcium Aluminate Dissolution.* Langmuir. 33 (2017) 45-55. https://doi.org/10.1021/acs.langmuir.6b03474

6. E. M. J. Bérodier, A. C. A. Muller, and K. L. Scrivener, *Effect of sulfate on C-S-H at early age.* Cement and Concrete Research. 138 (2020) 106248. https://doi.org/10.1016/j.cemconres.2020.106248

7. F. Zunino and K. Scrivener, *Factors influencing the sulfate balance in pure phase C_3S/C_3A systems.* Cement and Concrete Research. 133 (2020) 106085. https://doi.org/10.1016/j.cemconres.2020.106085

8. M. Maier, S. Scherb, A. Neißer-Deiters, N. Beuntner, and K.-C. Thienel, *Hydration of cubic tricalcium aluminate in the presence of calcined clays.* Journal of the American Ceramic Society. 104 (2021) 3619-3631. https://doi.org/10.1111/jace.17745

9. S. Scherb, M. Maier, N. Beuntner, K.-C. Thienel, and J. Neubauer, *Reaction kinetics during early hydration of calcined phyllosilicates in clinker-free model systems.* Cement and Concrete Research. 143 (2021) 106382. https://doi.org/10.1016/j.cemconres.2021.106382

10. M. Maier, R. Sposito, N. Beuntner, and K.-C. Thienel, *Particle characteristics of calcined clays and limestone and their impact on the early hydration and sulfate demand of blended cement.* Cement and Concrete Research. 154 (2022) 15. https://doi.org/10.1016/j.cemconres.2022.106736

11. A. Quennoz and K. L. Scrivener, *Interactions between alite and C_3A-gypsum hydrations in model cements.* Cement and Concrete Research. 44 (2013) 46-54. http://dx.doi.org/10.1016/j.cemconres.2012.10.018

12. L. Valentini, M. Dalconi, M. Favero, G. Artioli, and G. Ferrari, *In-Situ XRD Measurement and Quantitative Analysis of Hydrating Cement: Implications for Sulfate Incorporation in C–S–H.* Journal of the American Ceramic Society. 98 (2015) 1259-1264. 10.1111/jace.13401

13. F. Zunino and K. Scrivener, *The influence of the filler effect on the sulfate requirement of blended cements.* Cement and Concrete Research. 126 (2019) 105918. https://doi.org/10.1016/j.cemconres.2019.105918

14. D. Jansen, C. Naber, D. Ectors, Z. Lu, X. M. Kong, F. Goetz-Neunhoeffer, and J. Neubauer, *The early hydration of OPC investigated by in-situ XRD, heat flow calorimetry, pore water analysis and 1H NMR: Learning about adsorbed ions from a complete mass balance approach.* Cement and Concrete Research. 109 (2018) 230-242. https://doi.org/10.1016/j.cemconres.2018.04.017

15. S. Scherb, N. Beuntner, and K.-C. Thienel, *Reaction kinetics of the basic clays present in natural mixed clays*, in *Proceedings of the 2nd International Conference on Calcined Clays for Sustainable Concrete*, F. Martirena, A. Favier, and K. Scrivener, Editors. 2018, Springer: Dordrecht, Netherlands. p. 427-433. https://doi.org/10.1007/978-94-024-1207-9_69

16. R. Sposito, M. Maier, N. Beuntner, and K.-C. Thienel, *Evaluation of zeta potential of calcined clays and time-dependent flowability of blended cement with customized polycarboxylate-based superplasticizers.* Construction and Building Materials. 308 (2021) 125061. https://doi.org/10.1016/j.conbuildmat.2021.125061

17. DIN ISO 9277, Determination of the specific surface area of solids by gas adsorption - BET method, (2003), Beuth-Verlag, p. 19

18. DIN EN ISO 17892-3, Geotechnical investigation and testing - Laboratory testing of soil - Part 3: Determination of particle density, (2015), Beuth-Verlag, p. 21

19. DIN 18132, Soil, testing procedures and testing equipment - Determination of water absorption, (2012), Beuth-Verlag, p. 14

20. S. Scherb, N. Beuntner, K.-C. Thienel, and J. Neubauer, *Quantitative X-ray diffraction of free, not chemically bound water with the PONKCS method.* Journal of Applied Crystallography. 51 (2018) 1535-1543. https://doi.org/10.1107/S1600576718012888

21. T. Degen, M. Sadki, E. Bron, U. König, and G. Nénert, *The HighScore suite.* Powder Diffraction. 29 (2014) S13-S18. https://doi.org/10.1017/S0885715614000840

22. H. M. Rietveld, *Line profiles of neutron powder-diffraction peaks for structure refinement.* Acta Crystallographica. 22 (1967) 151-152. https://doi.org/10.1107/S0365110X67000234

23. H. M. Rietveld, *An Algol Program for the Refinement of Nuclear and Magnetic Structures by the Profile Method*, in *RCN*. (1969), Reactor Centrum Nederland.

24. D. Jansen, F. Goetz-Neunhoeffer, C. Stabler, and J. Neubauer, *A remastered external standard method applied to the quantification of early OPC hydration.* Cement and Concrete Research. 41 (2011) 602-608. https://doi.org/10.1016/j.cemconres.2011.03.004

25. N. V. Y. Scarlett and I. C. Madsen, *Quantification of phases with partial or no known crystal structures.* Powder Diffraction. 21 (2006) 278-284. https://doi.org/10.1154/1.2362855

26. S. T. Bergold, F. Goetz-Neunhoeffer, and J. Neubauer, *Quantitative analysis of C–S–H in hydrating alite pastes by in-situ XRD.* Cement and Concrete Research. 53 (2013) 119-126. http://dx.doi.org/10.1016/j.cemconres.2013.06.001

27. M. C. Neuburger, *Präzisionsmessung der Gitterkonstante von Silicium*, in *Zeitschrift für Kristallographie - Crystalline Materials*. (1935). p. 313.DOI: https://doi.org/10.1524/zkri.1935.92.1.313.

28. Á. G. De La Torre, S. Bruque, J. Campo, and M. A. G. Aranda, *The superstructure of C3S from synchrotron and neutron powder diffraction and its role in quantitative phase analyses.* Cement and Concrete Research. 32 (2002) 1347-1356. https://doi.org/10.1016/S0008-8846(02)00796-2

29. P. Mondal and J. W. Jeffery, *The crystal structure of tricalcium aluminate, $Ca_3Al_2O_6$.* Acta Crystallographica Section B. 31 (1975) 689-697. https://doi.org/10.1107/S0567740875003639

30. P. F. Schofield, C. C. Wilson, K. S. Knight, and I. C. Stretton, *Temperature related structural variation of the hydrous components in gypsum.* Zeitschrift für Kristallographie - Crystalline Materials. 215 (2000) 707. https://doi.org/10.1524/zkri.2000.215.12.707

31. S. A. Markgraf and R. J. Reeder, *High-temperature structure refinements of calcite and magnesite.* American Mineralogist. 70 (1985) 590-600.

32. V. A. Drits, B. B. Zviagina, D. K. McCarty, and A. L. Salyn, *Factors responsible for crystal-chemical variations in the solid solutions from illite to aluminoceladonite and from glauconite to celadonite.* American Mineralogist. 95 (2010) 348-361. https://doi.org/10.2138/am.2010.3300

33. M. Catti, G. Ferraris, and G. Ivaldi, *Thermal strain analysis in the crystal structure of muscovite at 700 °C.* European Journal of Mineralogy. 1 (1989) 625-632. https://doi.org/10.1127/ejm/1/5/0625

34. W. R. Busing and H. A. Levy, *Neutron Diffraction Study of Calcium Hydroxide.* The Journal of Chemical Physics. 26 (1957) 563-568. https://doi.org/10.1063/1.1743345

35. F. Goetz-Neunhoeffer and J. Neubauer, *Refined ettringite ($Ca_6Al_2(SO_4)_3(OH)_{12}\cdot 26H_2O$) structure for quantitative X-ray diffraction analysis.* Powder Diffraction. 21 (2005) 4-11. https://doi.org/10.1154/1.2146207

36. T. Runcevski, R. E. Dinnebier, O. V. Magdysyuk, and H. Pöllmann, *Crystal structures of calcium hemicarboaluminate and carbonated calcium hemicarboaluminate from synchrotron powder diffraction data.* Acta Crystallographica Section B. 68 (2012) 493-500. https://doi.org/10.1107/S010876811203042X

37. C. Hoffmann and T. Armbruster, *Clinotobermorite, Ca5[Si3O8(OH)]2 · 4 H2O - Ca5[Si6O17] · 5 H2O, a natural C-S-H(I) type cement mineral: determination of the substructure*, in *Zeitschrift für Kristallographie - Crystalline Materials*. (1997). p. 864.DOI: https://doi.org/10.1524/zkri.1997.212.12.864.

38. R. Allmann, *Refinement of the hybrid layer structure $[Ca_2Al(OH)_6]^+$ $[1/2SO_4\ 3H_2O]^-$.* Neues Jahrbuch für Mineralogie. 3 (1977) 136-144.

39. H. Pöllmann and J. Kuzel H., *PDF data sheet: 42-0062, Calcium Aluminum Sulfate Hydrate.* (1990): Mineralogical Institute of University Erlangen, ICDD Grant-in-Aid.

40. N. Beuntner and K.-C. Thienel, *Pozzolanic efficiency of calcined clays in blended cements with focus on the early hydration.* Advances in Cement Research. 34 (2022) 341-355. https://doi.org/10.1680/jadcr.21.00034

41. T. Matschei, B. Lothenbach, and F. P. Glasser, *The role of calcium carbonate in cement hydration.* Cement and Concrete Research. 37 (2007) 551-558. http://dx.doi.org/10.1016/j.cemconres.2006.10.013

42. T. Matschei, B. Lothenbach, and F. P. Glasser, *The AFm phase in Portland cement.* Cement and Concrete Research. 37 (2007) 118-130. http://dx.doi.org/10.1016/j.cemconres.2006.10.010

43. B. Lothenbach and M. Zajac, *Application of thermodynamic modelling to hydrated cements.* Cement and Concrete Research. 123 (2019) 105779. https://doi.org/10.1016/j.cemconres.2019.105779

44. S. Scherb, M. Köberl, N. Beuntner, K.-C. Thienel, and J. Neubauer, *Reactivity of Metakaolin in Alkaline Environment: Correlation of Results from Dissolution Experiments with XRD Quantifications.* Materials. 13 (2020) 18. https://doi.org/10.3390/ma13102214

45. Y. Briki, M. Zajac, M. B. Haha, and K. Scrivener, *Impact of limestone fineness on cement hydration at early age.* Cement and Concrete Research. 147 (2021) 106515. https://doi.org/10.1016/j.cemconres.2021.106515

46. S. T. Bergold, F. Goetz-Neunhoeffer, and J. Neubauer, *Interaction of silicate and aluminate reaction in a synthetic cement system: Implications for the process of alite hydration.* Cement and Concrete Research. 93 (2017) 32-44. http://dx.doi.org/10.1016/j.cemconres.2016.12.006

47. A. Tironi, A. N. Scian, and E. F. Irassar, *Blended cements with limestone filler and kaolinitic calcined clay: filler and pozzolanic effects.* Journal of Materials in Civil Engineering. 29 (2017) 8. doi:10.1061/(ASCE)MT.1943-5533.0001965

48. R. Sposito, N. Beuntner, and K.-C. Thienel, *Rheology, setting and hydration of calcined clay blended cements in interaction with PCE-based superplasticisers.* Magazine of Concrete Research. 73 (2021) 785-797. https://doi.org/10.1680/jmacr.19.00488

49. C. Hesse, F. Goetz-Neunhoeffer, and J. Neubauer, *A new approach in quantitative in-situ XRD of cement pastes: Correlation of heat flow curves with early hydration reactions.* Cement and Concrete Research. 41 (2011) 123-128. http://doi.org/10.1016/j.cemconres.2010.09.014

50. O. Canbek, C. Szeto, N. R. Washburn, and K. E. Kurtis, *A quantitative approach to determining sulfate balance for LC3.* CEMENT. 12 (2023) 100063. https://doi.org/10.1016/j.cement.2023.100063

51. F. Zunino and K. Scrivener, *Insights on the role of alumina content and the filler effect on the sulfate requirement of PC and blended cements.* Cement and Concrete Research. 160 (2022) 106929. https://doi.org/10.1016/j.cemconres.2022.106929

52. E. Pustovgar, R. K. Mishra, M. Palacios, J.-B. d'Espinose de Lacaillerie, T. Matschei, A. S. Andreev, H. Heinz, R. Verel, and R. J. Flatt, *Influence of aluminates on the hydration kinetics of tricalcium silicate.* Cement and Concrete Research. 100 (2017) 245-262. https://doi.org/10.1016/j.cemconres.2017.06.006

53. B. Mota, T. Matschei, and K. Scrivener, *The influence of sodium salts and gypsum on alite hydration.* Cement and Concrete Research. 75 (2015) 53-65. https://doi.org/10.1016/j.cemconres.2015.04.015

54. E. Potapova and E. Dmitrieva, *The effect of metakaolin on the processes of hydration and hardening of cement.* Materials Today: Proceedings. 19 (2019) 2193-2196. https://doi.org/10.1016/j.matpr.2019.07.373

55. C. Naber, S. Stegmeyer, D. Jansen, F. Goetz-Neunhoeffer, and J. Neubauer, *The PONKCS method applied for time resolved XRD quantification of supplementary cementitious material reactivity in hydrating mixtures with ordinary Portland cement.* Construction and Building Materials. 214 (2019) 449-457. https://doi.org/10.1016/j.conbuildmat.2019.04.157